

Ehsan Sharifi, Alpana Sivam, Sadasivam Karuppannan and John W Boland
Landsat surface temperature data analysis for urban heat resilience: case study of Adelaide

Planning Support Science for Smarter Urban Futures, 2017 / Geertman, S., Allan, A., Pettit, C., Stillwell, J. (ed./s), Ch.24, pp.433-447. Series: Lecture Notes in Geoinformation and Cartography

© Springer International Publishing AG 2017

The final publication is available at Springer via http://dx.doi.org/10.1007/978-3-319-57819-4_24

PERMISSIONS

<http://www.springer.com/gp/open-access/authors-rights/self-archiving-policy/2124>

Springer is a green publisher, as we allow self-archiving, but most importantly we are fully transparent about your rights.

Publishing in a subscription-based journal

By signing the Copyright Transfer Statement you still retain substantial rights, such as self-archiving:

*"Authors may self-archive the author's accepted manuscript of their articles on their own websites. Authors may also deposit this version of the article in any repository, provided it is only made **publicly available 12 months** after official publication or later. He/ she may not use the publisher's version (the final article), which is posted on SpringerLink and other Springer websites, for the purpose of self-archiving or deposit. Furthermore, the author may only post his/her version provided acknowledgement is given to the original source of publication and a link is inserted to the published article on Springer's website. The link must be provided by inserting the DOI number of the article in the following sentence: "The final publication is available at Springer via [http://dx.doi.org/\[insert DOI\]](http://dx.doi.org/[insert DOI])"."*

2 May 2018

<http://hdl.handle.net/2440/108130>

Chapter 24

Landsat Surface Temperature Data Analysis for Urban Heat Resilience: Case Study of Adelaide

Ehsan Sharifi*, **Alpana Sivam**, **Sadasivam Karuppanan**, **John Boland**

Abstract

This chapter demonstrates the application of Landsat 7 ETM+ and Landsat 8 surface cover-temperature data to support planning for urban heat resilience. Satellite data is used to analyse the correlation of the urban surface covers on surface heat island effect in Adelaide. Methods to identify best-fit satellite images, surface cover classification, surface temperature calculation and their cross-mapping are detailed. Results indicate that tree canopy and surface water covers had the least surface temperature variations in micro and mesoscale. Average minimum surface temperature of tree canopy cover was 2.79°C lower than asphalt and 4.74°C lower than paved areas. It is argued that freely available satellite urban surface temperature data analysis can assist urban planning authorities in planning heat resilient urban spaces in the context of climate change.

Keywords urban cover, land use, urban heat island, remote sensing, urban greenery

E. Sharifi (Corresponding author) •

School of School of Information Technology and Mathematical Sciences, University of South Australia, Adelaide, Australia

Email: ehsan.sharifi@unisa.edu.au

J. Boland

Email: john.boland@unisa.edu.au

A. Sivam

School of Art, Architecture and Design, University of South Australia, Adelaide, Australia

Email: alpana.sivam@unisa.edu.au

S. Karuppanan

Email: sadasivam.karuppanan@unisa.edu.au

1. Introduction

Cities are anticipated to accommodate up to 70% of the global population by 2050 (DESA 2014). Unlike the current urbanisation rate of 50%, almost all the expected global population growth will be accommodated in cities. Such rapid urbanisation means higher densities will be needed in existing cities and many new urban areas to accommodate up to 2 billion new urban dwellers. A considerable amount of natural landscape is transformed into buildings and hard surfaces, creating environmental threats to existing and future cities. Huge demands for natural resources in cities results in a contribution of up to 80% to the greenhouse gas (GHG) emissions (OECD 2010, UNECE 2011, UN-Habitat 2014).

Climate change projections indicate that – due to excessive GHG emissions – surface temperature in Australia is likely to increase 3.8°C by 2090 (CSIRO 2007). Such an increase in temperature will have a severe impact on natural ecosystems and human life in cities, including public health and quality of public space (Guest, Willson et al. 1999, Stone 2012). In the meantime, the built environment suffers from the effect of an additional form of heat, known as the urban heat island (UHI) effect. This human-made heat is trapped in built environment's thermal mass and can result in higher densities being significantly hotter, compared to their peri-urban counterparts. The urban-rural temperature difference frequently reaches 4°C and can peak at more than 10°C (Oke 1988, Gartland 2008, Wong, Jusuf et al. 2011). Such additional heat stress can seriously impact citizens' health and the quality of public life in cities.

This chapter demonstrates application of Landsat 7 ETM+ and Landsat 8 surface cover and thermal band data and discusses the use of urban thermal mapping in supporting urban planning and decision making to achieve resilience to heat in the built environment.

2. Background

Progressive literature on the UHI effect indicates that the artificial increase of temperature in cities is happening because of changes in radiative energy and water budget in the built environment (Coutts, Beringer et al. 2007, Errell, Pearlmutter et al. 2011, Santamouris and Kolokosta 2015). This artificial temperature increase affects urban microclimates in different layers of the atmosphere, including the surface layer (buildings and land surfaces), the canopy layer (below the canopy of trees or at human scale) and the boundary layer (up to 1500 metres above the ground surface) (Oke 1987). These three layers of urban microclimates are tangled in complex climatic systems, while local air circulation in the built environment can moderate the UHI effect by mixing the air in each layer with other adjacent layers.

Urban surface cover materials alter the magnitude of heat stress in the built environment. Impermeable and hard surfaces in cities tend to store more heat in their thermal mass during the day compared to natural landscapes. They emit stored heat during the night and cause the built environment to be relatively hotter than the rural counterparts – known as the urban heat island effect. Oke (2006) argues that the UHI effect has four major contributing factors:

- Urban geometry, which alters heat exchange balance in the built environment by affecting shadow and wind patterns. It affects the exposure of materials to sunlight and the consequent heat storage in thermal mass. This complex heat radiation exchange between building mass and adjacent atmosphere can also change the intensity and patterns of airflow in urban canyons.
- Urban cover and surface materials, which affect the heat absorption and reflection time-rate in the built environment. Thermodynamic specification, colour, texture and density of materials and their exposure to sunlight can alter the heat flux in outdoor spaces in complex procedures.
- Urban landscape affect water and heat exchange rate in the built environment. Photosynthesis and evaporation processes in urban greenery contribute to decrease the ambient temperature. Urban greenery typology, distribution and intensity also affect lower atmospheric air turbulence.
- Urban metabolism and anthropogenic (human made) waste heat in cities is mainly related to mass energy consumption for indoor air-conditioning and motorized transportation.

Existing literature on the UHI effect is mainly focused on monitoring and documentation of the UHI effect in macro (regional) scales. Research on the key contributors to the surface layer UHI (sUHI) effect at precinct scale can provide useful links between UHI investigations at city and meso scales.

The temperature in some Australian cities such as Sydney, Melbourne and Adelaide is already up to 4°C warmer than surrounding areas. This chapter investigate the case study of the City of Adelaide sUHI effect, which is an example of a city facing an increasing UHI effect due to its post-19th century style of urban development. Due to the city's temperate climate and the UHI effect, public spaces in Adelaide are increasingly warmer in summer than humans' thermal comfort, pushing citizens into air-conditioned buildings and creating an ever-increasing rise in outdoor temperatures.

3. Materials and methods

Satellite remote sensing data is used to analyse the mesoscale effect of the urban surface cover classes on surface heat island effect in Adelaide. Selected Landsat 7 and Landsat 8 images were obtained from USGS Global Visualization Viewer (<http://glovis.usgs.gov>) to facilitate analysis of urban surface temperature. Four satellite images between 2001-2002 and 2013-2014 covering the coldest and the hottest available remote sensing data in Adelaide, are used for surface cover and temperature analysis.

3.1 Selection criteria for satellite images

Satellite images were obtained in two different time spans of 2001-2002 and 2013-2014. Landsat 7 was launched in 1999 provides satellite images with thermal bands through its enhanced thematic mapper plus (ETM+) sensor. However, a defect in scan line corrector (SLC) of Landsat 7 ETM+ in May 2003 resulted in some partial data loss and parallel stripes in satellite images. Therefore, the Landsat 7 ETM+ data was only used from 2001 to 2002 in the analysis. Landsat 8 was launched in February 2013, and its data for 2013 to 2014 period was used in this research.


















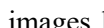
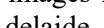
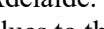
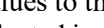
All the available satellite images were considered against the maximum acceptable threshold of 10% cloud coverage of the study area. Two Landsat 7 ETM+ images (captured in 2001-2002) and two Landsat 8 images (captured in 2013-2014) for the coldest and hottest days were chosen for further analysis. These best-fit images were selected based on maximum and minimum daily temperature of the images to present the coldest and hottest weather conditions during study periods (see Tables 1 and 2).

Selected satellite images were then assessed against heat stress, excess heat and climate normality conditions based on:

- average daily maximum and minimum temperature of three days before the date of the images to reflect heat stress intensity
- maximum and minimum average monthly temperature of the images to reflect normality of the date of images in respective months
- 30-years maximum and minimum average temperatures to reflect excess heat values

Thus, these selected satellite images represent the coldest and hottest available Landsat 7 and Landsat 8 surface temperature data for Adelaide metropolitan area and its inner suburbs. The images were analysed for their surface cover classification and surface temperature.

Table 1. Best-fit Landsat 7 ETM+ and Landsat 8 images for Adelaide that represent coldest (blue) and hottest (red) thermal images during 2001-2002 and 2013-2014 (weather data: Australian Bureau of Meteorology).

Date	Image ID	Min. Daily Temp. (°C)	Max. Daily Temp. (°C)	Mean Daily Temp. (°C)	Cloud cover
1/05/2001	LE70970842001005ASA00	16.9	27.4	 22.15	7% (0% CBD)
2/06/2001	LE70970842001037EDC00	20.5	36.5	 28.5	0%
22/2/2001	LE70970842001053ASA00	14.6	29.9	 22.25	0%
30/6/2001	LE70970842001181EDC00	3.3	15.5	 9.4	0%
18/9/2001	LE70970842001261EDC00	9.3	24.1	 16.7	0%
20/10/2001	LE70970842001293ASA00	5.9	20.4	 13.15	0%
23/12/2001	LE70970842001357EDC00	16.3	23.2	 19.75	2% (0% CBD)
24/1/2002	LE70970842002024ASA00	17.2	31.6	 24.4	3% (0% CBD)
25/2/2002	LE70970842002056EDC00	16.7	33.2	 24.95	0%
9/05/2002	LE70970842002248EDC00	8.2	22.8	 15.5	10% (0% CBD)
21/9/2002	LE70970842002264ASA00	9.9	25.2	 17.55	5% (0% CBD)
11/08/2002	LE70970842002312EDC00	14.6	26.5	 20.55	0%
27/9/2013	LC80970842013270LGN00	9.1	24.5	 16.8	3% (0% CBD)
14/11/2013	LC80970842013318LGN00	8.4	21.9	 15.15	3% (0% CBD)
30/11/2013	LC80970842013334LGN00	11.2	29.8	 20.5	0%
16/12/2013	LC80970842013350LGN00	11	30.4	 20.7	0%
2/02/2014	LC80970842014033LGN00	28.7	44.7	 36.7	1% (0% CBD)
3/06/2014	LC80970842014065LGN00	13.5	23.9	 18.7	0%
22/3/2014	LC80970842014081LGN00	11.2	22.6	 16.9	2% (0% CBD)
29/8/2014	LC80970842014241LGN00	7.8	24.7	 16.25	0%
12/03/2014	LC80970842014337LGN00	20.6	32.8	 26.7	3% (0% CBD)

As shown in Table 1, the targeted cold-labeled images have minimum daily temperature of 3.3°C (2001) and 7.8°C (2013) in Adelaide. Table 2 indicates the comparison of these minimum daily temperature values to the long-term 30-years minimum monthly temperature values in that the selected images are taken in typical cold days for their climate context. For the hot-labeled images the daily maximum temperature was 36.5°C (2001) and 44.7°C (2014) in Adelaide. A comparison of these minimum daily temperature values to long-term 30-years minimum monthly temperature values in Table 2 indicates that the selected images are taken in typical hot days for their climate context. Weather data were taken from the Australian Bureau of Meteorology official weather stations in Adelaide Kent Town (no. 23090).

Table 2 Heat stress and excess heat conditions for the selected best-fit Landsat 7 and Landsat 8 images for Adelaide (weather data: Australian Bureau of Meteorology).

Weather Condition	Season code	Date	Image ID	Min. Daily Temp. (°C)	Max. Daily Temp. (°C)	Mean Daily Temp. (°C)	Temp at 12:00pm (°C)	3-days before Min. Average Temp. (°C)	3-days before Max. Average Temp. (°C)	3-days before Mean Temp. (°C)	Lowest Temp. Month (°C)	Highest Temp. Month (°C)	Mean Monthly Min. Temp. (°C)	Mean Monthly Max. Temp. (°C)	Mean Monthly Temp. (°C)	Mean 30-years Monthly Min. Temp. (°C)	Mean 30-years Monthly Max. Temp. (°C)	Mean 30-years Monthly Temp. (°C)	Air Temp in the time of image (°C)
Hot	SUM	2/06/2001	LE70970842001037EDC00	21	37	28.5	30	20.9	31.8	26.4	13.8	40	20	32	25.8	17	29	23.4	23
Cold	WIN	30/6/2001	LE70970842001181EDC00	3.3	16	9.4	14	6	16.3	11.2	2.8	23.6	8.9	16	12.6	8.2	16	12.2	11
Hot	SUM	2/02/2014	LC80970842014033LGN00	29	45	36.7	41	21.8	39	30.4	10.7	44.7	18	30	23.8	17	29	23.4	30
Cold	WIN	29/8/2014	LC80970842014241LGN00	7.8	25	16.3	17	5.9	21.6	13.8	0.9	25	6.8	17	12.1	8.2	17	12.5	10

3.2 Urban surface covers classification

Urban heat island literature argues that surface cover materials alter the magnitude of heat stress in urban settings (Oke 1988, Tapper 1990, Gartland 2008, Ichinose, Matsumoto et al. 2008, Wong and Jusuf 2010, Santamouris, Gaitani et al. 2012). All GeoTIFF files except those related to the Panchromatic, Cirrus, Coastal Aerosol and Thermal Bands had to be processed. This includes B1, B2, B3, B4, B5, B7 layer-bands for Landsat 7 and B2, B3, B4, B5, B6, B7 layer-bands for Landsat 8. The number of bands dictate the maximum number of surface cover feature classes (six for this study). Urban surface cover materials were categorised under six classes as follows:

- Tree canopy class included tree canopies, bushes, and shrubs
- Grass cover class included grassland areas and other ground cover greeneries including shrubs
- Paving cover class included building rooftops, concrete and other paved areas with materials such as clay
- Asphalt cover class included asphalt and bitumen in streets and parking areas
- Natural-hard cover class included all bare surfaces, beaches, vacant lands and temporary hard-landscape covers without greenery
- Water feature class included surface water of rivers, sea, and urban water features

For every data set, these layer-bands were stacked together and classified in tree, grass, street, urban, land and water feature classes using supervised classification process of satellite images in ENVI software. For each cover class at least 20 areas covered dominantly by the targeted surface cover classes were used as

benchmarks (120 samples in total for each image). Classified surface covers are validated via cross-checking with Google Earth maps of the same area with similar timeframes. Emissivity and atmospheric correction of thermal data are applied in ArcGIS, and urban surface cover temperatures were calculated based on thermal bands 6 (Landsat 7) and 10 (Landsat 8). Resulting surface cover temperatures are compared to urban land cover classes.

3.3 Surface temperature extraction from multi-spectrum satellite data

An ideal thermal image for surface class-temperature measurement is to have match values of surface coverage and temperature for every identical pixel, meaning that the surface temperature is measured in the same area of surface cover classes. Thus, an ideal urban surface heat investigation depends on the simultaneous mapping of visible and thermal data in overlapped images. Such simultaneous RGB-NIR-Thermal mapping is available via Landsat 7 ETM+ and Landsat 8 satellite imagery.

Landsat 7 ETM+ (since 1999) and Landsat 8 (since 2013) provide surface temperature data from different spectral bands (see Table 3). For the evaluation of land surfaces temperatures in Landsat 7, the thermal infrared (TIR) channel (Band 6-1 from 10.31 μm to 12.36 μm) were used. Similar surface temperature data are available in the thermal infrared (TIRS) channel of Landsat 8 (Band 10 from 10.6 μm to 11.19 μm). The in-nadir resolution of the surface temperatures is 30m.

Satellite image data consist of digital numbers ranging from 0 to 255. Such digital numbers can be converted into degree Kelvin in three steps:

- calculation of radiance for digital number
- atmospheric correction
- calculation of degree Kelvin for the final radiance values (denoted the Planck function) and degree Kelvin to degree Centigrade conversion

The spectral radiation density of the thermal sensors was calculated in ENVI software. Since the surface temperatures of the emitting areas of the ground were the final objects of interest, two influences should be eliminated from the satellite images: the deviation of the surface from a “black body” and the influence of the atmosphere on the heat radiation.

The first step was handled by introducing an emissivity value (ϵ) between 0 and 1 for the reduction factor of real-body emission compared to the black-body (the emissivity value is commonly generalized to be 0.95 for large-scale urban surfaces). More accurate emissivity values for the selected surface cover classes in this study are suggested to be 0.91 for street, 0.90 for building rooftops (urban), 0.91 for open land and 0.98 for greenery (Nichol 1996, Voogt and Oke 2003, Weng, Lu et al. 2004, Coll, Galve et al. 2010).

Radiation gets absorbed when passing through transparent mediums such as the Earth's atmosphere, an atmospheric correction of the estimated radiances is required for more accurate surface temperature results, using the transmission values (τ) between zero and one that were obtained from Landsat 7 and Landsat 8 complementary metadata files. In the final step, the surface temperature in degree Kelvin were calculated from the corrected radiances using this formula (Li, Jackson et al. 2004, Coll, Galve et al. 2010):

(surface temperature calculation equation) (1)

$$T = \frac{K2}{\ln\left(\frac{K1}{L_y} + 1\right)}$$

T = at-satellite surface temperature (K)

K1= Band-specific thermal conversion constant from metadata (666.09 for Landsat 7 ETM+ B6; 774.89 for Landsat 8 B10)

K2 = Band-specific thermal conversion constant from metadata (1282.71 for Landsat 7 ETM+ B6; 1321.08 for Landsat 8 B10)

L_y = atmospherically corrected spectral radiance

$\ln()$ = natural logarithm function

Surface cover class reconstruction and temperature calculation were done via Exelis Visual Information Solutions (ENVI) software. Final representation of remote sensing data is carried out in Q-GIS and ARC-GIS software.

4. Results

Distribution of the urban surface covers temperature in Adelaide is presented in Figures 1 and 2. The surface temperature values are averaged and therefore, present the mean value of all pixels belong to each surface class in each image.

Sharifi, E., Sivam, A., Karuppanan, S., & Boland, J. (2017). Landsat Surface Temperature Data Analysis for Urban Heat Resilience: Case Study of Adelaide In S. Geertman, A. Allan, C. Pettit & J. Stillwell (Eds.), *Planning Support Science for Smarter Urban Futures* (pp. 433-448): Springer.

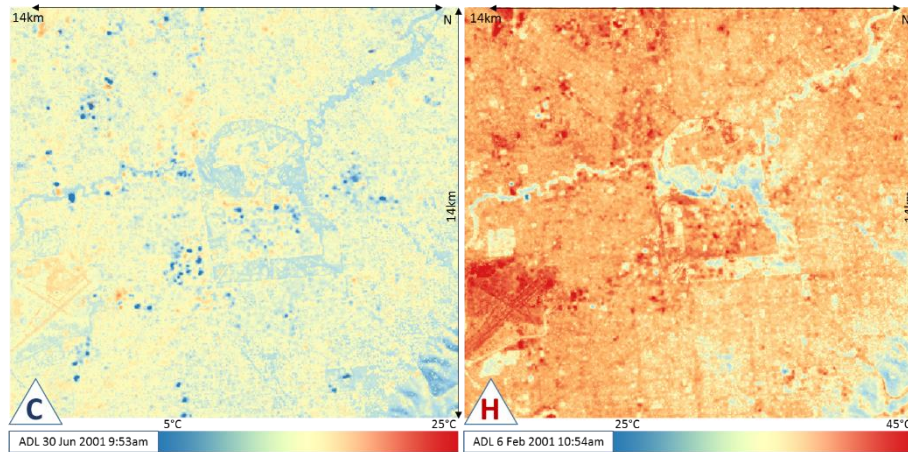


Figure 1 Surface temperature variation in cold (30 June 2001) and hot (6 February 2001) satellite images of Adelaide CBD and its inner suburbs – area: 14km × 14km (Map data: Landsat 7 ETM+ 2014)

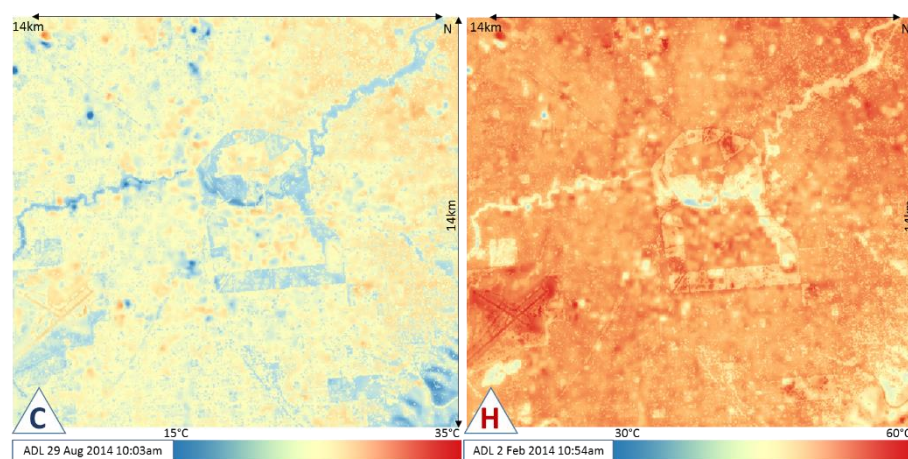


Figure 2 Surface temperature variation in cold (29 August 2014) and hot (2 February 2014) satellite images of Adelaide CBD and its inner suburbs – area: 14km × 14km (Map data: Landsat 8 2014)

Detailed variations in surface temperature of urban covers are presented in Table 3. The reported surface temperature of water in Adelaide is mostly related to the River Torrens. Therefore, a relatively higher surface water temperature is reported in Adelaide. Diurnal urban surface cover temperature tends to fluctuate more during the hot seasons (see the last column in Table 3). In other word, daily surface temperature of urban covers varies more when overall temperature is

higher, and hotter surface covers have more variation from the average urban temperatures.

Table 3 Average surface temperature of six urban land cover classes in Adelaide local council areas

Thermal Code	Satellite	local day	Tree canopy (°C)	Grass cover (°C)	Paving (°C)	Asphalt (°C)	Natural-hard (°C)	water (°C)	Air temp. (°C)	Max surface temp. variation from air temp. (°C)
C	L7	30-Jun-01	11.3	13.3	14.4	14.6	13.3	10.2	11.0	3.6
C	L8	29-Aug-14	21.0	23.4	25.1	25.2	23.8	18.5	10.0	15.2
H	L7	6-Feb-01	35.0	37.9	39.5	39.6	38.4	31.4	23.0	16.6
H	L8	2-Feb-14	38.5	41.3	43.0	43.3	41.8	34.3	30.0	13.3

Table 4 shows that tree canopy had the least surface minimum and maximum temperatures especially during hot seasons. The highest difference of 5.65°C was recorded between the surface temperature of tree canopy and artificial-hard landscapes including paving and asphalt (hot image of February 2001). Minimum surface temperature of tree canopy cover was at least 2.8°C lower than asphalt. Meanwhile, averaged maximum surface temperature of tree canopy was up to 4.1°C lower than asphalt and 4.0°C lower than paving cover. Due to close thermal characteristics of hard paving and asphalt in urban settings, these two cover classes are combined into artificial-hard landscape cover class in further discussion.

Surface water had the least fluctuating temperature due to high thermal capacity of water. Surface water temperature in Adelaide shows higher temperatures than expected due to its semi-isolation from large water volume of the sea. It mostly indicates the surface water temperature of slow-running river Torrens in the CBD area.

Paving and Asphalt had the most fluctuating and highest relative temperatures during the study. Grass cover had lower temperature variation in colder seasons, whereas showed very high temperature variations of 11.2°C in February 2014. The high variation of grass cover temperature in hot seasons is associated with its moisture and its level of irrigation.

Table 4 Detailed variations in surface temperature of urban covers in Adelaide during 2001-2002 and 2013-2014

		Tree canopy (°C)	Grass cover (°C)	Paving (°C)	Asphalt (°C)	Natural- hard (°C)	water (°C)
C	Min.	9	11.41	9.85	11.9	10.69	7.14
	Max.	13.47	15.28	16.51	16.55	15.27	12.26
	Var.	4.47	3.87	6.66	4.65	4.58	5.12
C	Min.	18.3	21.55	21.93	23.11	21.92	16.17
	Max.	23.18	25.31	27.23	27.19	25.9	20.61
	Var.	4.88	3.76	5.3	4.08	3.98	4.44
H	Min.	31.03	34.2	36.66	36.68	35.58	25.03
	Max.	40.67	43.15	43.3	43.31	42.14	32.43
	Var.	9.64	8.95	6.64	6.63	6.56	7.4
H	Min.	33.67	35.73	39.12	40.64	38.83	23.17
	Max.	43.81	46.96	45.82	46.15	44.59	34.19
	Var.	10.14	11.23	6.7	5.51	5.76	11.02

4.1.1 Normalised surface temperature (NST)

Variation in absolute surface temperature of six urban covers in Tables 3 and 4 reveals that tree canopy and surface water tend to have cooler surfaces during hot weather conditions. The temperature difference between surface covers and air temperature provides a better measure for comparison, since it decreases the effect of seasonal climate. A normalised surface temperature (NST) measure is suggested for further discussion (air temperature needs to be measured at 2-3m from the surface to avoid near-surface temperature effect).

$$\text{(normalised surface temperature (NST))} \quad (2)$$

$$NST = T_{\text{surface cover}} - T_{\text{air}}$$

As Figure 3 shows, surface water, and tree canopy have the lowest NST in the range. Surface water had the lowest NST value during heat stress conditions. It means that surface water is the most significant microclimate moderator in hot weather conditions. Application of surface water is limited in urban settings due to space availability, infrastructure requirements, and functional constraints.

The second best performance is related to tree canopy cover, which had 5°C (in average) lower NST than artificial-hard landscapes during hot weather conditions. Meanwhile, grass cover had 1.9°C (in average) lower NST than artificial-hard landscapes. Natural-hard landscape cover has a similar variation as grass cover in Adelaide. Average tree canopy cover was 11% cooler than hard-landscapes during

hot weather conditions in Adelaide. Thus, average tree canopy facilitates 13% lower surface temperatures compared with artificial-hard landscapes.

Tree canopy also had lower NST in cold weather. However, its averaged surface temperature was 4°C lower than artificial-hard landscape cover. As such, a surface temperature reduction of tree canopy cover is 1°C higher in hot weather compared to cold conditions. Thus, tree canopy cover contributes to outdoor temperature reduction in hot weather, while its temperature reduction is less significant in cold thermal environments.

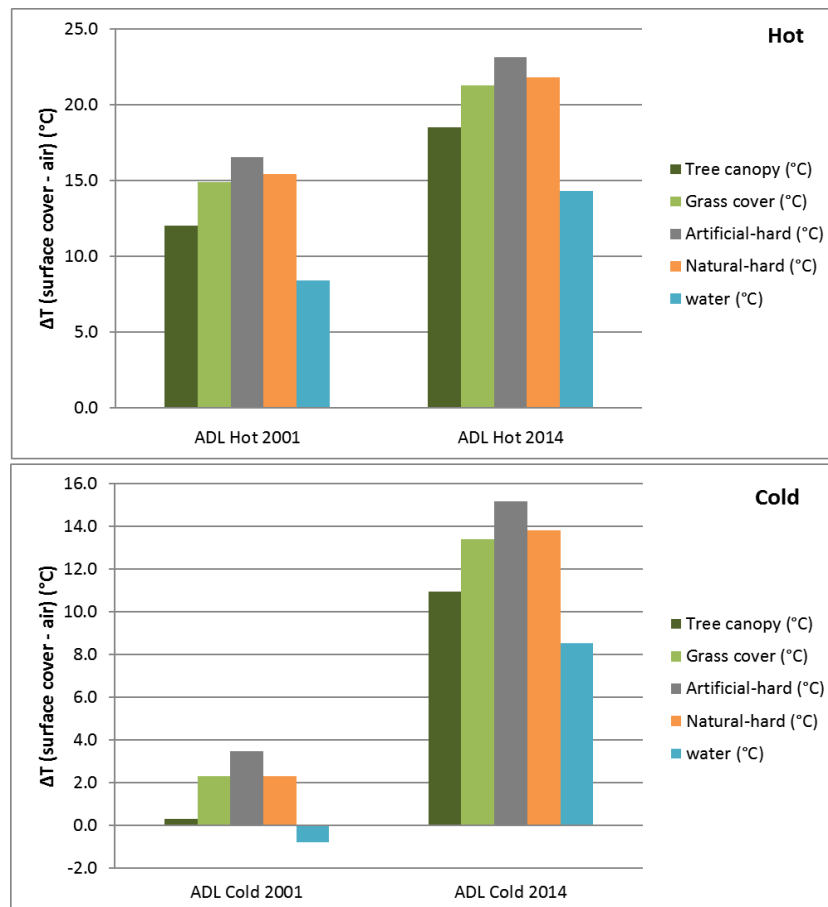


Figure 3 Normalised surface temperature of urban cover classes in hot and cold seasons in Adelaide (2001-2002 and 2013-2014)

5. Discussion

5.1. Urban transformation towards heat resilience

Urban development is a slow process and built environment comprising of housing, commercial, industrial and institutional buildings have a lifespan of several decades before substantial changes or redevelopment can occur. Australian cities are among the least densely populated cities in the world mainly due to urban sprawl (SoAC 2014-2015). However, with emphasis on more medium and high density housing and urban consolidation policies density is likely to increase marginally over the medium term. More and more existing old detached housing is gradually replaced with semidetached housing leading to increase in building footprint in urban areas. This is likely to increase surface temperature in critical summer months.

To some extent current planning and building guidelines exacerbate the issue of urban heat. For example, planning rules prescribe minimum open space standards for various types of dwelling on various lot sizes usually as percentage of the block area. The nature of open space – lawns and trees or concrete or stone paving – is not prescribed. This has led to concrete and stone paving on sides and rear of the property. The purpose of open space can be made effective towards mitigating urban heat island effect if limits on open space paving is imposed so that green surface cover on private land can be maintained in residential areas. Public spaces comprising of parks, open spaces, and roads and other transport networks together account for over one third of urban gross area. Water sensitive pavement design provide a useful solution to mitigate urban surface temperature and promote sub-soil water table in central parts of the city.

5.2. Application in urban policy making and design

The use of freely available satellite urban surface temperature data can assist urban planning authorities in formulating planning policy and regulation to plan and develop heat resilient urban spaces in the context of local climate and climate change. The results presented here demonstrate that materials used in building and urban spaces impact on urban surface temperature. In general, urban planning policies and regulations prescribe percentage of mandatory open space and ground coverage for various urban land uses.

Seldom planning regulations focus on percentage of hard surface and soft surface. The research highlights the role of various urban surface covers and it emerges that effective ways to minimise urban heat islands require planning norms and standards for hard surface covers such as paving and asphalt surfaces. Prescribing building coverage and open space as a ratio of block area alone would not address

the issue. Using urban surface temperature data for land uses planners could develop policy for various types of activity spaces to make cities more resilient. Urban surface temperature data will assist urban designer to create a land use pattern that could mitigate urban heat effects and adapt climate change. This will help create functional spaces that could increase space utilisation as well as reduce the need for artificial surface covers. Urban heat measurement and mitigation strategies need to be incorporated in urban policy making and development processes for more resilient urban futures.

6. Conclusions

Urban temperatures are predicted to increase due to climate change. The temperatures in our cities are likely to increase further, because more heat will be stored and re-radiated by expanses of asphalt, concrete and other heat-storing building materials. In this context, it is crucial to understand the possibilities for the transformation of existing urban fabrics towards a more liveable and sustainable future (Bosselmann 2008). This can be implemented by spatial transformation and heat-proofing interventions in existing urban spaces (Santamouris, Synnefa et al. 2011).

The basic argument underlined in this research is that the higher UHI effect at precinct scale correlates with a greater hard-landscaped public space ratio and a lower urban greenery ratio. Therefore, increasing urban greenery and decreasing hard-landscaped urban features such as conventional concrete, paving and asphalt covers can contribute to urban cooling in existing precincts, where a fine distribution of urban greenery could reduce the UHI effect.

Remote sensing surface temperature data analysis is a planning support tool to create a smarter and more resilient urban futures. Further research is required to explore how far can hard surface development be from vegetated or water surfaces to still benefit from the cooling effect of these land uses or if vegetation and water have to be closely integrated with development projects.

7. Research limitations and further opportunities

This research is based on remote sensed thermal images and analysis spatial data normally used by planners and urban designers. Remote sensing data analysis is subject to uncertainty due to invisible urban surfaces from satellite view such as surfaces under the tree canopy and vertical surfaces.

Sharifi, E., Sivam, A., Karuppanan, S., & Boland, J. (2017). Landsat Surface Temperature Data Analysis for Urban Heat Resilience: Case Study of Adelaide In S. Geertman, A. Allan, C. Pettit & J. Stillwell (Eds.), *Planning Support Science for Smarter Urban Futures* (pp. 433-448): Springer.

To move towards more certainty about the research outcomes, on-the-spot micro-climate measurement and urban surface mapping at smaller-scales could be beneficial. The results could also be validated in other cities in comparable climate conditions.

Local climate of cities affect heat transfer in the built environment. Therefore, application of research findings in cities with different climate regimes needs further investigation. This is also essential for generalisation of research findings.

This study utilises the surface temperature which is different from the real feeling of the temperature in public space. Further studies could benefit from including on-the-spot climate measurements and air temperature data. The effect of local airflow and surface water is subject to further investigation.

Sharifi, E., Sivam, A., Karuppanan, S., & Boland, J. (2017). Landsat Surface Temperature Data Analysis for Urban Heat Resilience: Case Study of Adelaide In S. Geertman, A. Allan, C. Pettit & J. Stillwell (Eds.), *Planning Support Science for Smarter Urban Futures* (pp. 433-448): Springer.

References

- Bosselmann, P. (2008). *Urban Transformation: Understanding City Design and Form*. Washington DC: Island Press.
- Coll, C., Galve, J. M., Sanchez, J. M. & Caselles, V. (2010). Validation of Landsat-7/ETM+ Thermal-Band Calibration and Atmospheric Correction With Ground-Based Measurements. *Geoscience and Remote Sensing* **48**(1), 547-555.
- Coutts, A., Beringer, J. & Tapper, N. J. (2007). Impact of Increasing Urban Density on Local Climate: Spatial and Temporal Variations in the Surface Energy Balance in Melbourne, Australia. *Journal of Applied Meteorology and Climatology* **46**(4), 477-493.
- CSIRO (2007). *Climate Change in Australia: Technical Report* Aspendale VIC, CSIRO and Australian Bureau of Meteorology.
- DESA (2014). *World Urbanization Prospects: Highlights*. Department of Economic and Social Affairs Population Division. New York, United Nations
- Erell, E., Pearlmutter, D. & Williamson, T. (2011). *Urban Microclimate: Designing the Spaces between Buildings*. London: Earthscan.
- Gartland, L. (2008). *Heat Islands: Understanding and Mitigating Heat in Urban Areas*. Washington, DC: Earthscan.
- Guest, C. S., Willson, K., Woodward, A. J., Hennessy, K., Kalkstein, L. S., Skinner, C. & McMichael, A. J. (1999). Climate and Mortality in Australia: Retrospective Study, 1979-1990, and Predicted Impacts in Five Major Cities in 2030. *CLIMATE RESEARCH* **13**(1), 1-15.
- Ichinose, T., Matsumoto, F. & Kataoka, K. (2008). Counteracting Urban Heat Islands in Japan. *Urban Energy Transition: From Fossil Fuels to Renewable Power*. D. Peter. Amsterdam, Elsevier, 365-380.
- Landsat 7 ETM+ (2014).
- Landsat 8 (2014).
- Li, F., Jackson, T. J., Kustas, W. P., Schmugge, T. J., French, A. N., Cosh, M. H. & Bindlish, R. (2004). Deriving Land Surface Temperature from Landsat 5 and 7 during SMEX02/SMACEX. *Remote Sensing of Environment* **92**(4), 521-534.
- Nichol, J. E. (1996). High-Resolution Surface Temperature Patterns Related to Urban Morphology in a Tropical City: A Satellite-Based Study. *Journal of Applied Meteorology* **35**(1), 135-146.
- OECD (2010). *Cities and Climate Change*. Paris: Organisation for Economic Cooperation and Development

Sharifi, E., Sivam, A., Karuppanan, S., & Boland, J. (2017). Landsat Surface Temperature Data Analysis for Urban Heat Resilience: Case Study of Adelaide In S. Geertman, A. Allan, C. Pettit & J. Stillwell (Eds.), *Planning Support Science for Smarter Urban Futures* (pp. 433-448): Springer.

- Oke, T. R. (1987). *Boundary Layer Climates*. New York: Wiley
- Oke, T. R. (1988). The Urban Energy Balance. *Progress in Physical Geography* **12**(4), 471-508.
- Oke, T. R. (2006). Initial Guidance to Obtain Representative Meteorological Observations at Urban Sites: Instruments and Observing Methods. IOM Report No. 81. Canada, World Meteorological Organization.
- Santamouris, M., Gaitani, N., Spanou, A., Saliari, M., Giannopoulou, K., Vasilakopoulou, K. & Kardomateas, T. (2012). Using Cool Paving Materials to Improve Microclimate of Urban Areas – Design Realization and Results of the Flisvos Project. *Building and Environment* **53**(0), 128-136.
- Santamouris, M. & Kolokosta, D. D. (2015). *Urban Microclimates: Mitigating Urban Heat*. *Low Carbon Cities*. S. Lehmann. New York, Routledge, 282-292.
- Santamouris, M., Synnefa, A. & Karlessi, T. (2011). Using Advanced Cool Materials in the Urban Built Environment to Mitigate Heat Islands and Improve Thermal Comfort Conditions. *Solar Energy* **85**(12), 3085-3102.
- SoAC (2014-2015). *State of Australian Cities*. Canberra, Department of Infrastructure and Transport, Commonwealth of Australia, Major Cities Unit.
- Stone, B. (2012). *City and the Coming Climate: Climate Change in the Places we Live*. New York: Cambridge University Press
- Tapper, N. J. (1990). Urban Influences on Boundary-Layer Temperature and Humidity - Results from Christchurch, New-Zealand. *Atmospheric Environment Part B-Urban Atmosphere* **24**(1), 19-27.
- UN-Habitat (2014). *Planning for Climate Change. A Strategic Values-based Approach for Urban Planners*. Cities and Climate Change London, United Nations Human Settlements Programme.
- UNECE (2011). *Climate Neutral Cities: How to Make Cities Less Energy and Carbon Intensive and more Resilient to Climatic Challenges*. New York and Geneva, United Nations Economic Commission for Europe.
- Voogt, J. A. & Oke, T. R. (2003). Thermal Remote Sensing of Urban Climates. *Remote Sensing of Environment* **86**(3), 370-384.
- Weng, Q., Lu, D. & Schubring, J. (2004). Estimation of Land Surface Temperature–Vegetation Abundance Relationship for Urban Heat Island Studies. *Remote Sensing of Environment* **89**(4), 467-483.
- Wong, N. H. & Jusuf, S. K. (2010). Study on the Microclimate Condition Along a Green Pedestrian Canyon in Singapore. *Architectural Science Review* **53**(2), 196-212.
- Wong, N. H., Jusuf, S. K. & Tan, C. L. (2011). Integrated Urban Microclimate Assessment Method as a Sustainable Urban Development and Urban Design Tool. *Landscape and Urban Planning* **100**(4), 386-389.